ELSEVIER

Journal of Hazardous Materials B128 (2006) 150–157

Journal of Hazardous Materials

www.elsevier.com/locate/jhazmat

Adsorption kinetics of malachite green onto activated carbon prepared from Tunçbilek lignite

Y. Önal [a,*], C. Akmil-Başar [a], Didem Eren [b], Çigdem Sarıcı-Özdemir [a], Tolga Depci [b]

[a] *Inonu University, Faculty of Engineering, Department of Chemical Engineering, 44280 Malatya, Turkey*
[b] *Inonu University, Faculty of Engineering, Department of Mining Engineering, 44280 Malatya, Turkey*

Received 19 April 2005; received in revised form 11 July 2005; accepted 29 July 2005
Available online 8 September 2005

Abstract

Adsorbent (T_3K618) has been prepared from Tunçbilek lignite by chemical activation with KOH. Pore properties of the activated carbon such as BET surface area, pore volume, pore size distribution, and pore diameter were characterized by *t*-plot based on N_2 adsorption isotherm. The N_2 adsorption isotherm of malachite green on T_3K618 is type I. The BET surface area of the adsorbent which was primarily contributed by micropores was determined 1000 m^2/g. T_3K618 was used to adsorb malachite green (MG) from an aqueous solution in a batch reactor. The effects of initial dye concentration, agitation time, initial pH and adsorption temperature have been studied. It was also found that the adsorption isotherm followed both Freundlich and Dubinin–Radushkevich models. However, the Freundlich gave a better fit to all adsorption isotherms than the Dubinin–Radushkevich. The kinetics of adsorption of MG has been tested using pseudo-first-order, pseudo-second-order and intraparticle diffusion models. Results show that the adsorption of MG from aqueous solution onto micropores T_3K618 proceeds according to the pseudo-second-order model. The intraparticle diffusion of MG molecules within the carbon particles was identified to be the rate-limiting step. The adsorption of the MG was endothermic (ΔH° = 6.55–62.37 kJ/mol) and was accompanied by an increase in entropy (ΔS° = 74–223 J/mol K) and a decrease in mean value of Gibbs energy (ΔG° = −6.48 to −10.32 kJ/mol) in the temperature range of 20–50 °C.

Keywords: Activated carbon; Adsorption; Reaction kinetics; Lignite; Malachite green

1. Introduction

Dyes removal of wastewater is the main problem encountered in textile industry. Although they are not particularly toxic, the dyes affect aquatic diversity by blocking the passage of light through the water. Since the effluents have complex nature, it is difficult to treat such stream by a single process and conventional physicochemical and biological treatment methods are not sufficient for adequate treatment. Liquid-phase adsorption processes have been shown to be highly efficient for removal of colors, odor, organic and inorganic pollutants from the industrial wastewater. This has created an interest concerning the use of activated carbon on this area. But its usage is limited due to its high cost and this has lead many researchers for cheaper sources to prepare activated carbon. Ru-Ling et al. [1] prepared activated carbon from pine wood at different activation times. They measured adsorption isotherm and rates of three dyes and three phenols at 30 °C. Rozada et al. [2] studied potential usage of activated carbon from sewage sludge for absorption of methylene blue and saphranine. They analyzed the pure and binary adsorption assay in batch and fixed bed systems. Al-Degs et al. [3] studied the effect carbon surface on the removal of reactive dyes from textile effluent. They obtained high adsorption capacity and it was attributed to the net positive surface charge which occurs during the adsorption process. Similarly, Manuel Fernando et al. [4] treated the commercial activated carbon chemically and thermally and it was shown that the surface chemistry of the activated carbon plays a key

* Corresponding author. Tel.: +90 422 341 00 10; fax: +90 422 341 00 46.
E-mail address: yonal@inonu.edu.tr (Y. Önal).

0304-3894/$ – see front matter © 2005 Elsevier B.V. All rights reserved.
doi:10.1016/j.jhazmat.2005.07.055

role in dye adsorption performance. Jain et al. [5] utilized the industrial waste products as adsorbents for the removal of dyes. They prepared a number of low cost adsorbents from steel and fertilizer industries and investigated the removal of anionic dyes from the aqueous solutions. It was found that the prepared adsorbents are 80% as efficient as activated charcoal and they can be used as low cost alternative. Chen et al. [6] used granular activated carbon prepared from different raw materials for the removal of 2-methylisoborneol from drinking water. Various adsorbents have been prepared from saw dust [7], rice husk [8], wheat straw, corncobs, barley husk [9,10], and plum kernels [11], a fresh water algae (*Phithophora* sp.) [12] and there are still many efforts on development of low cost materials with higher adsorption capacity [13–21].

The aim of the present work is to study the adsorption capacity of activated carbon (T_3K618) prepared from Tunçbilek lignite for dye (malachite green, MG) removal from aqueous solutions. The experimental data for adsorbed MG on T_3K618 were compared using two isotherm equations namely, Freundlich and Dubinin–Radushkevich (D–R). Three adsorption kinetics models were tested in this study. To investigate the mechanisms of MG sorption, characteristics constants of adsorption were determined using a pseudo-first- and second-order equation, intraparticle diffusion respectively, and compared. In addition, the equilibrium thermodynamic parameters are determined for the MG on activated carbon.

2. Experimental

2.1. Materials

The dye, malachite green, CI = 42,000, chemical formula = $C_{50}H_{52}N_4O_8$, FW = 927.03, λ_{max} = 617 nm (reported) and λ_{max} = 617 nm (experimental obtained by us) was supplied by Merck (1398). An amount of 2000 mg/L stock solution was prepared by dissolving the required amount of dye in double distilled water. Working solutions of the desired concentrations were obtained by successive dilutions.

2.2. Preparation of activated carbon

Brought in containers from Tunçbilek–Kütahya (Turkey) lignite was dried under laboratory conditions for 3 h and then sieved to −60 + 100 mesh fraction and later stored in colorful plastic tubes. All experiments carried out with dried lignite at 105 °C. Adsorbent (T_3K618) were prepared from lignite by chemical activation with KOH, activation temperature and KOH/lignite ratio (impregnation ratio) was selected 800 °C and 4:1, respectively. The impregnated sample was raised to the activation temperature under N_2 (100 mL/min) atmosphere with 10 °C/min flow rate and hold at impregnation temperature for 1 h. After the activation, the sample was cooled down under N_2 flow and washed several times successively with hot distillated water until a neutral residue is obtained. The washed sample was dried at 110 °C to prepare activated carbon.

2.3. Instrumentation

The spectrophotometric determination of dye was done on a Shimadzu UV–vis spectrophotometer (Model UV-2100S). The pH of solutions was measured by using microprocessor based pH meter (Hanna Instruments pH 211). The pore structures of active carbon were investigated by using the standard Micromeritics DFT plus software. Nitrogen adsorption was recorded at 77 K by means of a TriStar 3000 (three port) surface analyzer (Micromeritics, USA). BET equation was used to calculate the specific surface area. Before the measurement, all samples were degassed at 300 °C for 3 h.

2.4. Adsorption experiments

Dye solutions were prepared in distilled water at desired concentrations. Adsorption experiments were carried out by agitating 0.1 g of T_3K618 with 25 mL dye solutions of desired concentration, pH and temperature in a thermostatic bath operating at 400 rpm. The pH of the dye solutions was adjusted with HCl or NaOH solution by using a pH meter. The amount of dye adsorbed onto T_3K618, q_t (mg/g), was calculated by mass-balance relationship equation (1):

$$q_t = (C_0 - C_t)\frac{V}{W} \quad (1)$$

where C_0 and C_t are the initial and time t liquid-phase concentration of the dye (mg/L), respectively, V the volume of the solution (L) and W the weight of the dry T_3K618 used (g).

3. Results and discussion

3.1. Characterization of the prepared adsorbent

Fig. 1 shows N_2 adsorption isotherm of the activated carbon (T_3K618) obtained using KOH reagent. N_2 adsorption

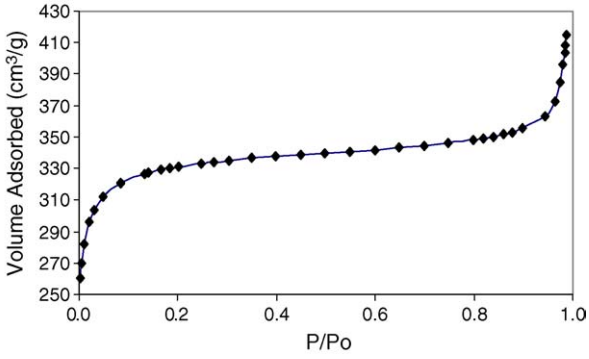

Fig. 1. Adsorption isotherm of nitrogen at 77 K for activated carbon (T_3K618).

Table 1
Surface area and porosity of the activated carbon

S_{BET} (m^2/g)	S_{ext}		S_{mic}		V_t (cm^3/g)	V_{mic}		D_p (nm)
	m^2/g	% of S_{ext}	m^2/g	% of S_{mic}		cm^3/g	% of V_{mic}	
1000	153	15.3	848	84.8	0.59	0.44	74.6	2.27

isotherm is classified as type I, characteristics of microporous solids, in IUPAC classification [22]. Table 1 contains the BET surface area (S_{BET}), external surface area (including mesopores and macropores area S_{ext}), micropores surface area (S_{mic}), total pore volume (V_t) and average pore diameter (D_p) results obtained by applying the BET equation to N_2 adsorption at 77 K and DR equation to N_2 adsorption at 77 K. It was found that the activated carbon had a remarkable BET surface area, which was primarily contributed by micropores. The average pore diameter was 2.3776 nm, indicative of its micropores character.

Fig. 2 shows the pore size distribution was calculated in the standard manner by using BJH method [23]. It appears that activated carbon was dominantly micropores. Percentage of micropores area is 84.8%.

3.2. Effect of temperature and concentration of dye on adsorption

Effect of temperature and dye concentration on removal of dye by activated carbon (T_3K618) is presented in Fig. 3. The percentage of dye removal increased from 61.78 to 85.17 as the adsorption temperature was increased from 20 to 50 °C for 2000 mg/L dye concentration. The fact that the adsorption increases with an increase in temperatures indicates the increase in the mobility of large dye molecules with increasing temperatures and the ongoing adsorption process is endothermic [24,25]. Dye concentrations 250, 500, 750, 1000, 1500, 2000 mg/L were selected in this study. The percentage of dye removal decreased for all dye concentration while dye concentration increases.

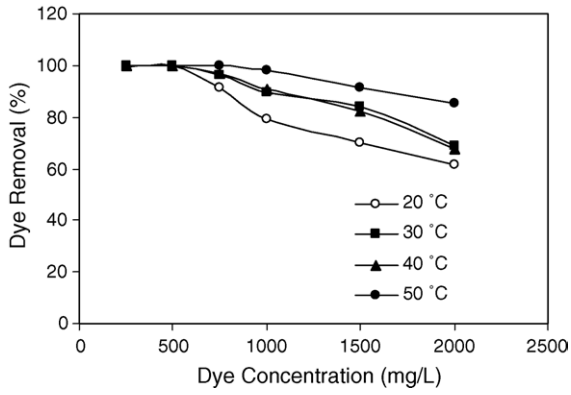

Fig. 3. Effect of initial dye concentration on malachite green removal by T_3K618 (adsorbent dosage = 0.1 g/25 mL, contact time = 3 h, pH = natural, at 400 rpm).

3.3. Effect of initial pH on adsorption

The magnitude of electrostatic charges imparted by ionized dye molecules is primarily controlled by the pH of medium. The amount of dye adsorbed or rate of adsorption tends to vary with pH of aqueous medium.

The experimental result of the adsorption of MG on T_3K618 as a function of pH at an initial dye concentration of 1500 mg/L, temperature 20 °C and 0.1 g adsorbent dosage is shown in Fig. 4. The percentage dye removal increases from 42 to 100 with increase in pH from 2 to 10. Maximum removal of dye was observed at around pH 5 and beyond that pH it attains the same maximum value. Since no significant change in the adsorbed amount of dye was observed after pH 5. It was suggested that the increase in adsorption depended

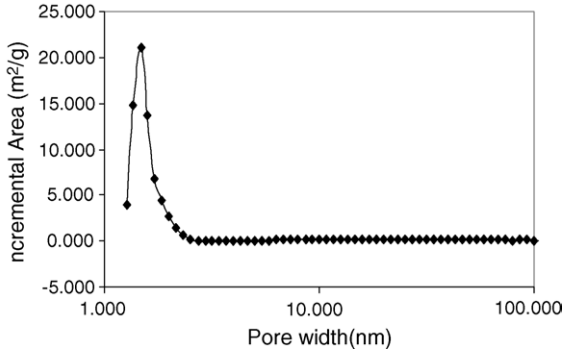

Fig. 2. Pore size distribution of the T_3K618.

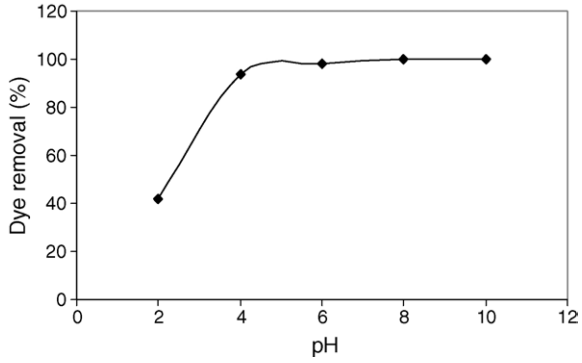

Fig. 4. Effect of pH on malachite green by T_3K618 (adsorbent dosage = 0.1 g/25 mL, temperature = 20 °C, at 400 rpm, contact time = 3 h).

on the properties of the adsorbent surface and the dye structure. Malachite green is a cationic triarylmethane dye. The results indicates that the protonation of MG occur in acidic medium.

And with the rise in pH the dye becomes more and more de-protonated. The low adsorption of dye also exhibits possibility of development of positive charge at activated carbon particles, which inhibits the adsorption of dye. However, the formation of electric double layer changes its polarity in the basic medium. Consequently, the dye removal increases. This result consists with literature [26].

3.4. Effect of contact time on adsorption

Adsorption experiments were carried out for different contact time at different temperature with a fixed adsorbent dosage of 0.1 g at natural pH. The results are presented in Fig. 5. Similar plots were determined. The adsorption percentage of dye increased with increase in contact time. The equilibrium time was 120 min for all adsorption temperature. The removal of dye is rapid in the initial stages of contact time and gradually decreases with lapse of time until saturation. The removal curves are single, smooth and continuous, indicating monolayer coverage of dye on the outer interface of the adsorbent initially [27].

3.5. Adsorption isotherms

The adsorption equilibrium data were fitted for Langmiur, Freundlich and Dubinin–Radushkevich (D–R) isotherms. The isotherm results indicate that the adsorption of MG onto T_3K618 is consistent with the Freundlich and Dubinin–Radushkevich isotherms.

The Freundlich adsorption isotherm can be expressed [28] as

$$\log q_e = \log k_f + \frac{1}{n} \log C_e \quad (2)$$

where q_e is the amount of dye adsorbed at equilibrium time (mg/g), C_e is the equilibrium concentration of the dye in solution (mg/L), k_f (L/g) and n are isotherm constant which indicate the capacity and intensity of the adsorption, respectively.

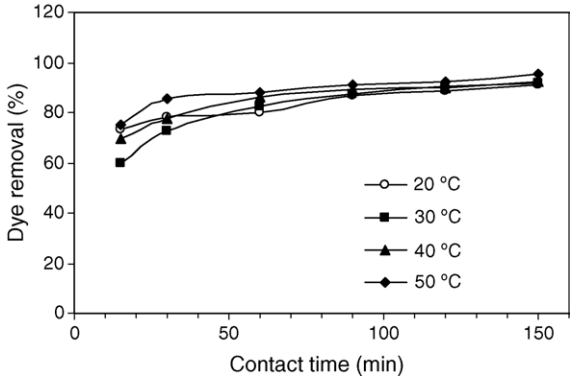

Fig. 5. Effect of contact time on malachite green removal by T_3K618 at different temperature (adsorbent dosage = 0.1 g/25 mL, pH = natural, at 400 rpm).

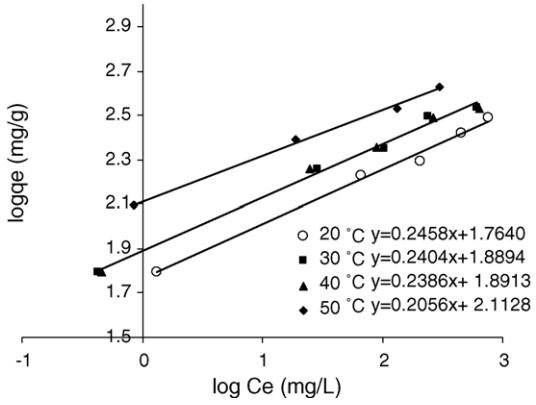

Fig. 6. Freundlich plots corresponding to the adsorption of malachite green on T_3K618 at different temperature.

Fig. 6 shows the plot of $\log q_e$ versus $\log C_e$ at 20, 30, 40, 50 °C adsorption temperature. The plot is in harmony with Freundlich isotherm. The values of k_f and n were calculated from the slope and intercept of the plot of $\log q_e$ versus $\log C_e$.

The D–R equation can be expressed [24] as

$$q_e = X'_m \exp(-K'\varepsilon^2) \quad (3)$$

where ε (Polanyi potential) is equal to $RT\ln(1 + 1/C_e)$, q_e is the amount of the dye adsorbed per unit activated carbon (mol/g). X'_m the adsorption capacity (mol/g), C_e the equilibrium concentration of the dye solution (mol/L), K' the constant of the adsorption energy ($mol^2\ kJ^2$), R the gas constant (kJ/mol K), and T the temperature (K). The linear form of the D–R isotherm is

$$\ln q_e = \ln X'_m - K'\varepsilon^2 \quad (4)$$

The plot of $\ln q_e$ versus ε^2 at 20, 30, 40, 50 °C adsorption temperature is presented in Fig. 7. The plot is in harmony with the D–R adsorption model. The values of X'_m and K' were calculated from intercept and slope of this plots. The constants obtained for Freundlich and D–R isotherms are shown in Table 2.

Table 2 shows an increase in adsorption capacity (k_f) with increase in temperature. A similar result is reported in the

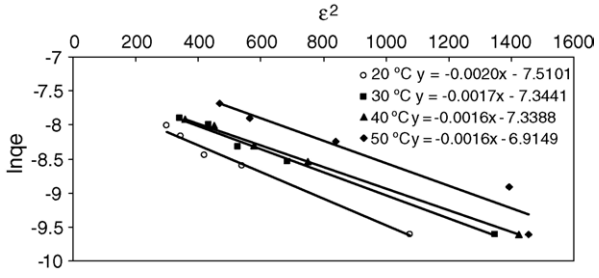

Fig. 7. Dubinin–Radushkevich isotherm of MG onto T_3K618 at different temperatures.

Table 2
Isotherm constant for the adsorption of MG onto T_3K618 at different adsorption temperature

Temperature (°C)	Freundlich isotherm			D–R isotherm		
	k_f (L/g)	n	r^2	X'_m (mol/g)	K' (mol^2 kJ^2)	r^2
20	58.08	4.068	0.993	5.48×10^{-4}	0.002	0.985
30	77.51	4.159	0.993	6.46×10^{-4}	0.0017	0.989
40	77.85	4.191	0.991	6.50×10^{-4}	0.0016	0.997
50	129.66	4.863	0.997	9.92×10^{-4}	0.0016	0.926

literature [26]. Values, $n > 1$ represent favourable adsorption condition [29]. The results suggest that the MG is favourably adsorbed by activated carbons prepared from lignite. In addition, the positive values for isotherm constant in case of T_3K618 signifies the monolayer adsorption and fits reasonably well with the Freundlich model indicating heterogeneous surface binding also [26,30].

X'_m, the adsorption capacity (mol/g), increases and K', the constant of the adsorption energy (mol^2 kJ^2), decreases with increasing temperature. The percentage of dye removal reaches maximum value at 50 °C.

It is important to mention that in the present studies, Freundlich model fits slightly better than the D–R model. This result has been recorded for other similar results in the literature [25].

3.6. Adsorption kinetics

Several kinetics models are used to examine the controlling mechanism of adsorption process such as chemical reaction, diffusion control and mass transfer. Applying those models given in literature [24,31–34].

The pseudo-first-order equation is expressed [23,30–34] as:

$$\frac{dq_t}{dt} = k_1(q_e - q_t) \quad (5)$$

After integration, the integrated form of Eq. (5) becomes:

$$\log(q_e - q_t) = \log q_e - \frac{k_1}{2.303}t \quad (6)$$

where q_e and q_t are the amounts of dye adsorbed (mg/g) at equilibrium and time t (min), respectively, and k_1 is the rate constant of pseudo-firs-order adsorption (min^{-1}).

The pseudo-second-order kinetic model of Ho and McKay [36,37] is

$$\frac{dq_e}{dt} = k_2(q_e - q_t)^2 \quad (7)$$

The integrated form of Eq. (7) becomes:

$$\frac{t}{q_t} = \frac{1}{k_2 q_e^2} + \frac{1}{q_e}t \quad (8)$$

where k_2 is the rate constant of pseudo-second-order adsorption (g/mg min) and $h = k_2 q_e^2$, where h is the initial adsorption rate (mg/g min).

The rate parameter for intraparticle diffusion is determined using the following equation [38]

$$q_t = k_{int} t^{1/2} + C \quad (9)$$

where C is the intercept and k_{int} is the intraparticle diffusion rate constant (mg/g min$^{1/2}$). The plot may present multilinearity, indicating that three steps take place. The first, sharper portion is attributed to the diffusion of adsorbate through the solution to the external surface of adsorbent or the boundary layer diffusion of solute molecules. The second portion describes the gradual adsorption stage, where intraparticle diffusion is rate limiting. The third portion is attributed to the final equilibrium stage [39].

First, the values of $\log(q_e - q_t)$ were calculated from the kinetic data of Fig. 5. The plots of $\log(q_e - q_t)$ versus t for the pseudo-first-order model given in Eq. (6) were given at different solution temperature in Fig. 8. The k_1 values were calculated from slope of this plot.

Second, the plots of (t/q_t) versus t for the pseudo-second-order model given in Eq. (8) were drawn at different solution temperature in Fig. 9. The q_e and k_2 values were calculated from slope and intercept of this plots, respectively.

Third, the intra particle diffusion rate, obtained from the plots q_t versus $t^{1/2}$. The plots are shown in Fig. 10. The external surface sorption (stage 1) is absent because of completion before 5 min. Initial linear portion (stage 2) followed by a plateau (stage 3). The initial linear portion of this plot is attributed to intraparticle diffusion. k_{int} values are determined from the slope of initial linear portion of this plot. The values of intercept, C give an idea about the boundary layer thickness, i.e. the larger the intercept, the greater is the boundary layer effect. The boundary layer diffusion depends on sev-

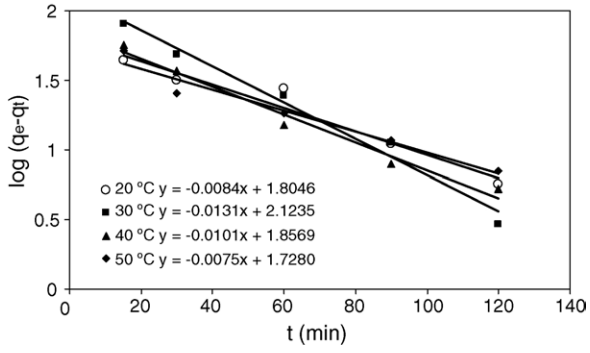

Fig. 8. Plots adsorption kinetic equation for adsorption of MG onto T_3K618, the pseudo-first-order adsorption kinetics of MG at different temperatures.

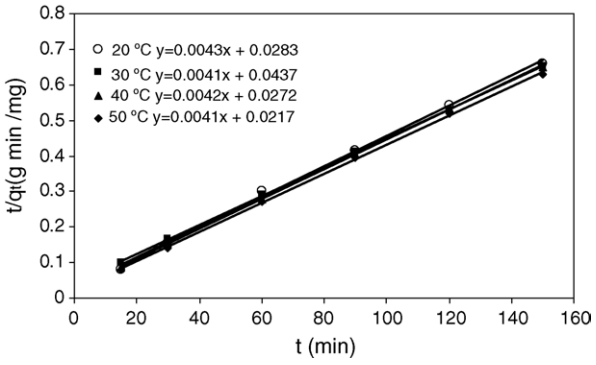

Fig. 9. Plots adsorption kinetic equation for adsorption of MG onto T_3K618, the pseudo-second-order adsorption kinetics of MG at different temperatures.

eral parameters, including the external surface area of the adsorbent, which is mainly controlled by the particle size, the shape and density of the particles, the concentration of the solution and the agitation velocity. The greater the particle size, the intraparticle diffusion resistance is the great in the control of the sorption kinetics of low-porous materials [40]. Our sample has high porosity (microporous). k_{int} values increases with increase of temperature that is why mobility of dye molecules increases. However, C (boundary layer thickness) values decrease with increase k_{int} values and temperature.

Kinetic parameters for three kinetic model and correlation coefficient were summarized in Table 3.

Table 3 shows that the correlation coefficients of second-order kinetic model are greater than those of other rate laws. Also, the calculated q_e values agree very well with the experimental data ($q_{e\,exp}$). These indicate that the adsorption perfectly complies with pseudo-second-order reaction [35]. Similar kinetic results have also been reported in literature [23,35].

3.7. Adsorption thermodynamics

Effect of concentration and temperature on the MG adsorption is shown in Fig. 3. While temperature increases, the percentage of dye removal increases slightly. The change in standard free energy (ΔG°), enthalpy (ΔH°) and entropy (ΔS°) of adsorption were calculated from the following equation:

$$\Delta G^\circ = -RT \ln K_c \tag{10}$$

where R is the gas constant, K_c the equilibrium constant and T the temperature in K. The K_c value is calculated from Eq. (11)

$$K_c = \frac{C_{Ae}}{C_{Se}} \tag{11}$$

where C_{Ae} and C_{Se} is the equilibrium concentration of dye ions on adsorbent (mg/L) and in the solution (mg/L) respectively.

Standard enthalpy (ΔH°) and entropy (ΔS°), of adsorption can be estimated from van't Hoff equation given in

$$\ln K_c = \frac{-\Delta H^\circ_{ads}}{RT} + \frac{\Delta S^\circ}{R} \tag{12}$$

The slope and intercept of the van't Hoff plot is equal to $-\Delta H^\circ_{ads}/R$ and $\Delta S^\circ/R$, respectively (23). The van't Hoff

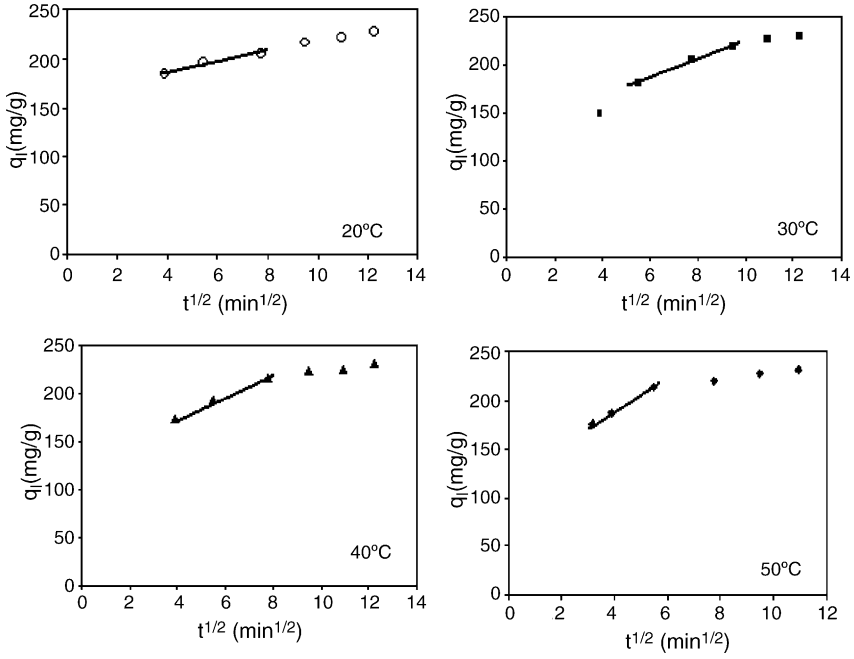

Fig. 10. Plots adsorption kinetic equation for adsorption of MG onto T_3K618, the intraparticle diffusion kinetics of MG at different temperatures.

Table 3
Kinetic parameters for the effects of solution temperature

Temperature (°C)	$q_{e\,exp}$ (mg/g)	First-order kinetic equation			Second-order kinetic equation			Intraparticle diffusion equation		
		q_e (mg/g)	k_1 ($\times 10^2$ min^{-1})	r^2	q_e (mg/g)	k_2 ($\times 10^4$ g/mg min)	r^2	k_{int} (mg/g min$^{1/2}$)	C	r^2
20	227.3	63.8	1.93	0.952	232.5	6.534	0.998	5.47	163	0.97
30	229.8	132.9	3.02	0.983	243.9	3.846	0.999	9.50	130	0.99
40	230.5	71.9	2.03	0.977	238.1	6.485	0.999	10.80	132	0.99
50	238.5	53.5	1.73	0.955	243.9	7.747	0.999	16.13	124	0.99

$q_{e\,exp}$: obtained as experimental.

plot for the adsorption of MG onto T_3K618 is given in Fig. 11. Thermodynamic parameters obtained are summarized in Table 4.

It is seen in Table 4 that the ΔH° values were in 6.55–62.37 kJ/mol with a mean value of 32.20 kJ/mol. The positive values of enthalpy change conform to the endothermic nature of the adsorption process. The positive values of ΔS° reflects the affinity of adsorbent material towards MG. The entropy (ΔS°) values vary from 74 to 223 J/mol K. Mean value of entrophy is 133 J/mol K. Similar results for endothermic adsorption of MG were also observed earlier on activated carbon prepared from de-oiled soya [24]. Despite being endothermic nature, the spontaneity of the adsorption process was decreased in the Gibbs energy of the system. The ΔG° values varied in range with the mean values showing a gradual increase from −6.48 to −10.32 kJ/mol in the temper-

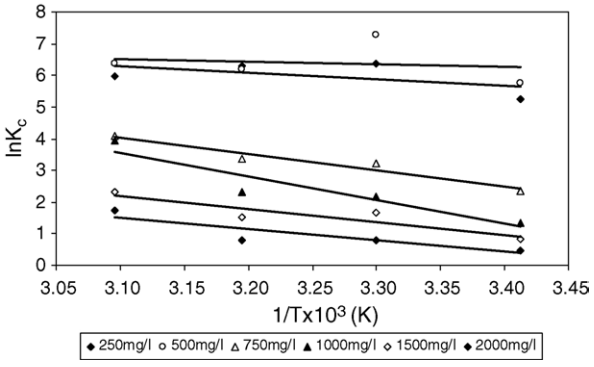

Fig. 11. van't Hoff plots of MG adsorption onto T3K618 for initial dye concentration at natural pH.

Table 4
Thermodynamic parameters for the adsorption of MG onto T_3K618

Concentration (mg/L)	Temperature (°C)	K_c	$-\Delta G^\circ$ (kJ/mol)	ΔH° (kJ/mol)	ΔS° (J/mol K)
250	20	189.02	12.77	17.42	106
	30	583.93	16.04		
	40	536.17	16.35		
	50	394.56	16.05		
500	20	319.08	14.04	6.55	74
	30	1447.01	15.16		
	40	493.12	16.14		
	50	585.23	17.11		
750	20	10.35	5.69	43.06	167
	30	25.20	8.13		
	40	29.20	8.78		
	50	60.57	11.02		
1000	20	3.79	3.25	62.37	223
	30	8.68	5.44		
	40	10.02	5.99		
	50	51.17	10.57		
1500	20	2.32	2.04	34.27	125
	30	5.21	4.15		
	40	4.65	3.99		
	50	10.21	6.24		
2000	20	1.62	1.17	29.55	105
	30	2.24	2.03		
	40	2.08	1.91		
	50	5.74	4.69		

ature range of 20–50 °C in accordance with the endothermic nature of the adsorption process.

4. Conclusion

The results of this work can be summarized as follows:

(1) The N_2 adsorption isotherm of malachite green on T_3K618 is of type I. The values of S_{BET}, V_t and S_{mic} and V_{mic} are 1000 m^2/g, 0.59 cm^3/g and 848 m^2/g, 0.44 cm^3/g, respectively. Results show that activated carbon is dominantly micropores. Percentage of micropores area is 84.8%.
(2) T_3K618 is a promising adsorbent for removal of MG from water. A small amount (4 g/L) of the adsorbent could almost decolorize an aqueous solution MG (500 mg/L) agitated for 3 h.
(3) Maximum removal of dye was observed at pH ∼5. Adsorption experiments were carried out for different contact time at different temperature with a fixed adsorbent dosage of 0.1 g/25 mL at natural pH. The equilibrium time was 120 min for all adsorption temperature.
(4) The adsorption isotherm followed Freundlich and Dubinin–Radushkevich models. The Freundlich gave a better fit to all adsorption isotherms (at 20, 30, 40, 50 °C) than the Dubinin–Radushkevich. Freundlich capacity (k_f) increases with an increase in adsorption temperature.
(5) The kinetics of adsorption of MG on T_3K618 was studied by using three kinetic models. The adsorption of MG from aqueous solution onto micropores T_3K618 proceeds according to the pseudo-second-order model which provides the best correlation of the data in all cases. The dye uptake process was found to be controlled by external mass transfer at earlier stages and by intraparticle diffusion at later stages.
(6) The adsorption of the dye, malachite green, was found to be endothermic indicating that the adsorption would be enhanced at temperature above the ambient temperature.

Acknowledgement

The author wishes to thank the (DPT K120330) Planning Organization Center for support.

References

[1] T. Ru-Ling, W. Feng-Chin, J. Ruey-Shin, Carbon 41 (2003) 487.
[2] F. Rozada, L.F. Calvo, A.I. García, J. Martín-Villacorta, M. Otero, Bioresour. Technol. 87 (2003) 221.
[3] Y. Al-Degs, M.A.M. Khraisheh, S.J. Allen, M.N. Ahmad, Water Res. 34 (2000) 927.
[4] R.P. Manuel Fernando, F.S. Samanta, J.M.O. José, L.F. José, Carbon 41 (2003) 811.
[5] A.K. Jain, V.K. Gupta, Bhatnagar, A. Suhas, J. Hazard. Mater. 101 (2003) 31.
[6] G. Chen, B.W. Dussert, I.H. Suffet, Water Res. 31 (1997) 1155.
[7] V.K. Garg, R. Gupta, A.B. Yadav, R. Kumar, Bioresour. Technol. 89 (2003) 121.
[8] K.S. Low, C.K. Lee, Bioresour. Technol. 61 (1997) 121.
[9] T. Robinson, B. Chandran, P. Nigam, Bioresour. Technol. 85 (2003) 119.
[10] T. Robinson, B. Chandran, P. Nigam, Bioresour. Technol. 84 (2002) 299.
[11] J. Ruey-Shin, W. Feng-Chin, T. Ru-Ling, J. Colloid Interf. Sci. 227 (2000) 437.
[12] K.V. Kumar, S. Sivanesan, V. Ramamurthi, Process Biochem. 40 (2005) 2865.
[13] K. Young Gun, C. Ung Su, K. Jeong Su, P. Yong Sung, Carbon 40 (2002) 2661.
[14] S. Zhemin, W. Wenhua, J. Jinping, Y. Jianchang, F. Xue, P. An, J. Hazard. Mater. 84 (2001) 107.
[15] A. Gurusamy, J. Ruey-Shin, L. Duu-Jong, Adv. Environ. Res. 6 (2002) 191.
[16] K.G. Vinod, S.K. Srivastava, T. Renu, Water Res. 34 (2000) 1543.
[17] P. Pendleton, S.H. Wong, R. Schumann, G. Levay, R. Denoyel, J. Rouquero, Carbon 35 (1997) 1141.
[18] A. Gurusamy, J. Ruey-Shin, L. Duu-Jong, J. Hazard. Mater. 92 (2002) 263.
[19] C. Namasivayam, D.J.S.E. Arasi, Chemosphere 34 (1997) 401.
[20] Rajeshwarisivaraj, V. Subburam, Bioresour. Technol. 85 (2002) 205.
[21] C. Grégorio, Bioresour. Technol. 90 (2003) 193.
[22] K.W. Sing, D.H. Everet, R.A.W. Haul, L. Moscou, R.A. Pierotti, J. Rouquero, T. Siemieniewasa, Pure Appl. Chem. 57 (1985) 603.
[23] P.E.P. Barrett, L.G. Joyner, P.P. Halenda, J. Am. Chem. Soc. 73 (1951) 373.
[24] B. Acemioğlu, J. Colloid Interf. Sci. 274 (2004) 371.
[25] A. Mittal, L. Krishnan, V.K. Gupta, Separation Purif. Technol. 43 (2) (2005) 125.
[26] V.K. Gupta, A. Mittal, L. Krishnan, V. Gajbe, Separation Purif. Technol. 40 (2004) 87.
[27] C. Namasivayam, K. Thamaraiselvi, R.T. Yamuna, Pest. Sci. 41 (1994) 7.
[28] H.M.F. Freundlich, Z. Phys. Chem. 57 (1906) 385.
[29] C. Namasivayam, K. Thamaraiselvi, R.T. Yamuna, Waste Manage. 14 (1993) 643.
[30] T. Robinson, B. Chandran, P. Nigam, Bioresour. Technol. 85 (2002) 119.
[31] C. Namasivayam, D. Kavitha, Dyes and Pigments 54 (2002) 47.
[32] M. Özacar, I.A. Sengil, Process Biochem. 40 (2005) 565.
[33] A. Bhatnagar, A.K. Jain, J. Colloid Interf. Sci. 281 (2005) 49.
[34] P.K. Malik, Dyes and Pigments 56 (2003) 239.
[35] Z. Aksu, Biochem. Eng. J. 7 (2001) 79.
[36] Y.S. Ho, G. McKay, Chem. Eng. J. 70 (1998) 115.
[37] Y.S. Ho, G. McKay, Process Biochem. 34 (1999) 451.
[38] W.J. Weber Jr., J.C. Morris, J. Saint, Eng. Div. Am. Soc. Civil Eng. 89 (1963) 2.
[39] E. Lorenc-Grabowska, G. Gryglewicz, J. Colloid Interf. Sci. 284 (2005) 416.
[40] N. Kannan, M.M. Sundaram, Dyes and Pigments 51 (2001) 25.